Research Square

Preprints are preliminary reports that have not undergone peer review.
They should not be considered conclusive, used to inform clinical practice,
or referenced by the media as validated information.

Effect of Liquid Metal Velocity during Low-Pressure Casting on the Microstructure and Mechanical Properties of Al12Si Alloy

Tansel TUNÇAY

tanseltuncay@karabuk.edu.tr

Karabük University

Abdulsefa CİN

Karabük University

Badegül TUNÇAY

Sivas University of Science and Technology

Derya DISPINAR

SINTEF Industry

Research Article

Keywords: Al-Si alloy, low-pressure casting, mechanical properties

Posted Date: November 17th, 2026

DOI: https://doi.org/10.21203/rs.3.rs-10727707/v1

License: This work is licensed under a Creative Commons Attribution 4.0 International License.
Read Full License

Additional Declarations: No competing interests reported.

Abstract

In this study, low-pressure die casting (LPDC) of the Al12Si (LM6) alloy was experimentally fabricated. For the Al12Si alloy, the velocity of the liquid metal in the gate cross sectional area was selected as 0.25, 0.50, and 1.00 m/s. To ensure the liquid metal's velocity, the metal was injected into the mould cavity using the required Argon gas, in accordance with Bernoulli's principle. Microstructural investigations and mechanical properties of an Al12Si alloy at different liquid metal velocities were evaluated. Microstructural analyses were performed using optical microscopy (OM) and scanning electron microscopy (SEM). Tensile and hardness tests were applied as mechanical tests. In microstructural examinations, it was determined that Al dendrites morphologically changed from linear-colonial to star-shaped as the liquid metal velocity increased. In addition, it has been determined that, during the solidification process under pressure, the liquid metal velocity and the Al-Si eutectic yield finer grains and a decrease in porosity. According to the density test results, the highest density was 2,465 g/cm³ at a liquid metal velocity at the gate of 0.5 m/s, and the lowest was 2,324 g/cm³ at a liquid metal velocity at the gate of 0.25 m/s. The change in hardness values could not be determined. According to the average tensile test results, the highest tensile strength was obtained at a liquid metal velocity at the gate of 0.5 m/s, 143 MPa (4.47% elongation), and the lowest tensile strength was obtained at a liquid metal velocity at the gate of 0.25 m/s, 125 MPa (3.48% elongation).

1. Introduction

LPDC is a casting process in which liquid metal is transferred into a metallic mould using argon or nitrogen gas, typically at a pressure of 0.3–0.5 bar, thereby ensuring laminar flow. During most LPDC operations, the applied gas pressure is maintained on the melt delivered into the mould cavity until solidification is complete. LPDC is widely used in the production of automotive components requiring high integrity, most notably wheels and cylinder heads, as well as in the aerospace industry. The transfer of liquid metal into the mould cavity in low-pressure die casting offers several important advantages, including high automation. Although the process generally involves a longer cycle time than gravity-fed permanent mould casting systems, a single operator can usually oversee multiple LPDC units simultaneously.

Furthermore, LPDC achieves a metal yield of approximately 80–95%, which is considerably higher than that of gravity casting processes, where yields are typically limited to 50–75% due to gating losses and the need for larger feeders. As with gravity casting methods, the use of sand cores does not normally pose difficulties, provided the pressure applied during melt transfer is carefully controlled. However, if excessive pressure is applied sometimes an effort to prevent the opening of bifilm oxide layers associated with microporosity sintering between the sand cores and the liquid metal may occur. Clearly, when the liquid metal is of sufficiently high quality, excessive driving pressure is unnecessary for suppressing porosity [1–3].

The LPDC method reveals several advantages over other casting methods. Mainly, the requirement for runner and sprue design is eliminated, and depending on the cast part, even the feeders can be eliminated. Therefore, the yield is significantly higher in LPDC castings. On the other hand, the most critical parameter in LPDC castings is the liquid's laminar flow in the mould cavity. In gravity castings, the sprue and runner must be designed to prevent turbulence during filling. Yet the best gravity designs include counter-gravity filling into the mould, because the free fall of liquid towards gravity always carries the risk of turbulence. Bonollo et al. [4] reported that LPDC has a higher yield than gravity due to the elimination of runners and feeders. The LPDC process enables the production of castings with very good soundness and defect-free surfaces.

In this sense, the LPDC method will always offer the best mould filling features, with the critical velocity of 0.5 m/s easily controlled by the pressure applied during filling [5]. Zhang et al. [6] casting defects: From a production point of view, cosmetic defects relating to hydrogen-based porosity and oxide films are the most critical. Du et al. [7] reviewed the importance of improved filling and controlled cooling during solidification in LPDC. Baghani et al. [8] studied the importance of the critical velocity in LPDC and demonstrated how to eliminate oxide film entrainment during LPDC. Dai et al. used simulation tools to investigate free-surface tracking.

Numerical simulations show that the number and distribution of oxide bifilm defects generated during filling are significantly affected by ingate velocity. Reducing ingate velocity effectively reduces casting defects [9]. Qiu et al. [10] reported studying different pressures and filling velocities. Used a simulation to show folding. Found a correlation between cross-section and inlet velocity. They claimed that even at a 0.5 m/s filling velocity, bifilms could be entrained, thereby reducing mechanical properties. Actually, the findings of that work were not related to filling velocity but to the quality of the starting melt, which appeared low. Song et al. [11] simulated the folded oxides and bifilms during filling, compared with experimental casting, to locate these defects in the microstructure. Sun et al. [12] oxides bifilms were detected in the LPDC casting of engine blocks. Mould filling and turbulence must be eliminated by optimizing using tools such as simulation prior to casting. Yang et al. [13] developed a numerical model to simulate entrained surface oxide films during the filling of aluminum castings. Ou et al. [14]simulated the process by acquiring comprehensive data, including extensive temperature measurements at different locations (die, wheel, and cooling channels), pressure in the cooling channels, and the size and location of shrinkage porosity in the produced wheels; subsequently, they attempted to validate the obtained data using a model and a simulation program [15].

In this study, a low-pressure casting system was designed and fabricated, and the effects of different argon pressures, corresponding to target liquid metal velocities of 0.25, 0.50, and 1.00 m/s, on the microstructural evolution and mechanical properties of the Al12Si alloys were systematically investigated.

2. Material and method

In the present study, Al12Si alloy was cast using the fabricated low-pressure casting machine at different melt velocities of 0.25, 0.50, and 1.0 m/s. A schematic view of the designed and manufactured low-pressure casting machine is presented in Fig. 1. The system comprises two independent heating units. The first is the melting furnace control unit used for liquid metal preparation, and the second is the control unit used to heat the metallic moulds fabricated from St 52-grade steel. These heating units operate with separate power supplies. The melting unit, fitted with a 1.5 mm resistance wire, has an approximate power rating of 4 kW, whereas the steel mould heating unit has a power rating of 3.75 kW. The melting unit was designed to melt approximately 1 kg of aluminum and its alloys within 1 h. A two-stage gas pressure regulator was used to reduce the pressure from the argon cylinder and to deliver the gas to the liquid metal surface at a constant flow rate. The inlet gas pressure could be adjusted in the range of 0-230 bar, whereas the outlet pressure was controllable between 0 and 1 bar with 0.1 bar intervals.

The dimensions of the steel moulds, fabricated from ST52 steel and designed to produce six tensile test specimens in a single casting operation, are shown in Fig. 2. a, whereas a photographic view of the moulds is provided in Fig. 2. b. To minimize mould surface erosion caused by the liquid metal during casting and to prevent elemental transfer by diffusion, the mould surfaces were spray-coated with a BH coating. Furthermore, a BN-coated graphite vertical runner was employed to convey the liquid metal, melted in the furnace system of the low-pressure casting machine, from the BN-coated stainless steel sheet crucible into the metallic mould cavity. The BN-coated graphite vertical runner had an inner diameter of 10 mm and an outer diameter of 20 mm.

Tuncel Metal San. supplied the Al12Si alloy ingots used in the present study. Each ingot weighed 17 kg. Chemical composition analysis of the ingots was carried out using a GNR S3 miniLAB300 optical emission spectrometer in the Department of Metallurgical and Materials Engineering, Faculty of Engineering and Natural Sciences, Karabuk University. The chemical composition of the as-received Al12Si alloy before casting is given in Table 1.

Table 1
Chemical composition of Al12Si alloy ingot before casting.

Elements (% wt.)								
Al	Si	Fe	Cu	Mg	Mn	Cr	Ti	Ni
87.463	12.523	0.002	0.002	0.001	0.002	0.002	0.001	0.002

In this study, a casting temperature of 720°C, approximately 150°C above the eutectic composition (577°C) in the Al-Si phase diagram, was used for the Al12Si alloy. When the Al12Si alloy reached the casting temperature, a graphite lance was immersed in a Foseco NITRAL 10MG degassing tablet (approximately 0.01% of the liquid metal's weight) and degassed for 10 minutes. Then, the pressure required to convey the liquid metal into the mould cavity at velocities of 0.25, 0.50, and 1.0 m/s in the nozzle cross-sectional area was calculated using the Bernoulli equation and the principle of

conservation of mass, and the results are given in Table 2. In addition, the metal mould (ST52 steel) was heated to 200°C and maintained at that temperature during casting. The velocities of liquid metal and applied pressures of the Al12Si alloy in the gating system are given in Table 2. Microstructure examinations were performed using a NIKON (Epiphot 200) optical microscope with Clemex Elite image processing program (OM) and a CARL ZEISS Ultra Plus Gemini FESEM (SEM) instrument. Mechanical tests were conducted using a SHIMADZU tensile testing machine (at a speed of 1 m/s) and an AFFRI macrohardness tester (2.5 mm steel ball and 31.25 kg/f force). Hardness values were repeated 5 times and averaged. Density tests were performed according to Archimedes' principle using a density kit on a Precisa XB200h precision balance with a sensitivity of 1/10000.

Table 2
Velocities of liquid metal and applied pressures of Al12Si alloy in the gating system.

Velocities of liquid metal	**Pressure applied to the liquid metal (mbar)**		
(m/s)	**0.080**	**0.125**	**0.20**
in vertical runner	1.05	2,11	3.175
in gate	0.25	0.50	1.00
in the mould cavity	0.16	0.32	0.48

3. Results and discussion

3.1 Chemical analysis results and discussions

Chemical analyses were performed on Al12Si alloys produced at different casting a liquid metal velocity at the gate after casting to control for possible contamination. Table 3 shows the chemical analyses of Al12Si alloys produced at different casting a liquid metal velocities at the gate. It was determined that the BN paint protection prevented the diffusion of the Fe element from the surface of the stainless-steel crucible into the liquid metal during melting.

Table 3
Chemical analyses of Al12Si alloy produced at different liquid metal velocities.

Al12Si	Elements (% wt.)								
	Al	Si	Fe	Cu	Mg	Mn	Cr	Ti	Ni
0.25 m/s	87.568	12.42	0.002	0.002	0.001	0.002	0.002	0.001	0.002
0.50 m/s	87.458	12.53							
1.00 m/s	87.468	12.52							

3.2 Microstructure results and discussions

Al12Si alloys produced by LPDC at different liquid metal velocities were examined using optical microscopy (OM) and scanning electron microscopy (SEM). Furthermore, the fracture morphology at the fracture surfaces after tensile testing was re-examined using SEM. OM images of Al12Si alloy produced by low-pressure casting at different liquid metal velocities are given in Fig. 3. According to the OM images at 10X magnification, α-Al dendrite arms and the surrounding Al-Si eutectic are observed. As the casting a liquid metal velocities at the gate increases, in the Al-Si alloy cast at 0.25 m/s, the Al dendrites solidify as longer and linear (columnar) grains, while in the Al-Si alloy cast at 0.5 m/s, shorter Al dendrites are visible, and at 1.00 m/s, much shorter α-Al dendrites oriented in different directions in a star-snowflake shape are noticeable. OM images at 50X magnification show that the eutectic Al-Si morphology is almost similar at a liquid metal velocities at the gate of 0.25 m/s and 0.50 m/s, but becomes thinner at 1.000 m/s.

Furthermore, OM images indicated that porosity in the casting decreased with increasing casting a liquid metal velocity at the gate. Yousefian and Tiryakioğlu [22] state that pore formation does not involve nucleation but is purely a growth mechanism. They further explain that aluminum casting porosity does not form via classical nucleation mechanisms; instead, pores form from the inflation of entrained oxide films (bifilms) that form during casting. Li et al.[16] cooling and microstructure are important. Porosity decreased by cooling.

Puga et al. examined the effectiveness of casting and ultrasonic degassing in the low-pressure casting of A356 alloy. Their results showed that ultrasonic degassing at lower temperatures promoted grain refinement of the primary α-Al phase more effectively than higher-temperature degassing, resulting in spherical grains with finer grain sizes. In addition, they reported that the gas pressure governing the casting rate, and thus the mould filling velocity, plays a crucial role in the formation of oxide films entrapped in the melt after solidification. They further suggested that oxide formation can be suppressed by using pressurisation curves that yield melt velocities below 0.5 m/s [17]. Timelli et al. [18] observed that the coarsening of the eutectic Si particles is observed by increasing the pressurising a liquid metal velocity at the gate. “eutectic Si exhibits a fibrous morphology for the analyzed pressure ramps with coarser particles by decreasing the filling time, i.e., increasing the pressurising a liquid metal velocity at the gate”. It can be established that, with increasing filling a liquid metal velocity at the gate, the microstructure is characterized by slightly coarser eutectic Si, whereas with reduced flow rate, the formation of a large number of fine Si particles is predominant. The impact of the filling time, within the analyzed range, on the morphology of eutectic Si is negligible. Therefore, an increase in filling a liquid metal velocity at the gate is more closely related to particle size than to aspect ratio.

The SEM images (Fig. 4) and EDS results (Table 4) of the Al12Si alloy produced by low-pressure casting at different liquid metal velocities indicate that variations in liquid metal velocity did not result in significant grain refinement of the primary α-Al phase. In addition, Si was detected at location 3 in the sample cast at 0.25 m/s, at locations 3 and 4 in the sample cast at 0.5 m/s, and at location 4 in the sample cast at 1.00 m/s. These results suggest that, within the range of casting conditions examined in

the present study, liquid metal velocity had no pronounced effect on the refinement of the primary α-Al phase, although localized compositional variations were identified in specific regions.

Comparable findings have been reported in the literature. Chiesa et al. investigated the low-pressure casting of A356 alloy in both sand and metallic moulds and found that alloys cast in permanent moulds exhibited higher tensile strength and ductility than those cast in sand moulds, mainly due to their shorter solidification times [19]. They also reported that directional solidification could be achieved in metallic moulds, whereas multidirectional solidification occurred in sand moulds. Furthermore, it has been shown that the microstructural evolution of the liquid metal in the mould cavity under constant pressure for 10 s is closely related to the applied pressure, and that increasing pressure promotes the formation of shorter dendrites. In this respect, the SEM micrographs of the Al12Si alloys produced at different liquid metal velocities, presented in Fig. 4, provide further evidence of the relationship between melt transfer conditions and the resulting microstructure. Papanikolaou et al. examined the optimization of counter-gravity casting, a process analogous to low-pressure casting, and emphasized the critical role of inlet velocity in determining casting quality [20]. Their results showed that stable liquid metal filling at very low inlet velocities increased the likelihood of surface defects, misruns, and premature solidification.

In contrast, proper control of inlet velocity enabled the production of higher-quality castings. They further noted that the velocity during the initial filling stage had a more dominant influence on final casting quality than that during the later stages, particularly when the free surface area of the liquid metal was large. In the present study, EDS analyses obtained at 500× magnification from SEM images of Al12Si alloys produced at different casting velocities are presented in Table 4, while the corresponding SEM images are shown in Fig. 4. Consistent with previous reports, the literature indicates that aluminum alloys produced by low-pressure casting under excessively low pressure may be susceptible to defects such as surface folding, oxide film formation, and incomplete mould filling due to premature solidification [21, 22]. Therefore, although lower filling velocities may contribute to a more stable filling pattern under certain conditions, excessively low melt velocities may negatively affect mould filling behavior and, consequently, the integrity of the final casting.

Table 4
EDS analysis results of Al12Si alloy produced by the low-pressure casting method at different liquid metal velocities.

Liquid metal velocities (m/sn)	Location	Al	Si	Fe	Mg	O
0.25	1	96.19	1.15	0	0.63	2.03
	2	65.80	31.47	0.38	0.56	1.79
	3	57.70	39.50	0	0.54	2.26
	4	92.81	13.89	0.51	0.55	2.24
	5	87.72	2.93	5.06	0.56	3.70
	6	95.78	1.17	0	0.77	2.28
0.50	1	95.25	1.87	0	0.66	2.22
	2	95.63	2.45	0	0.67	1.25
	3	40.07	57.71	0.19	0.49	1.54
	4	47.19	50.96	0	0.30	1.55
	5	64.89	32.40	0.67	0.52	1.56
	6	94.47	1.49	1.88	0.64	1.52
1.00	1	94.35	2.31	0	0.84	2.49
	2	94	1.50	0.38	0.89	3.23
	3	91.46	5.78	0	0.65	2.11
	4	58.74	38.71	0	0.34	2.22
	5	92.53	3.58	0.25	0.74	2.90
	6	95.43	1.67	0	0.66	2.23

3.3 Mechanical properties and discussions

Tensile test specimens were fabricated from Al12Si alloy parts produced by low-pressure casting at different liquid-metal velocities, in accordance with ASTM E8/E8M. Figure 5 shows the casting specimens, prepared tensile test specimens, and density specimens. Table 5 presents the tensile test results.

Table 5 presents the Weibull analysis data for the tensile test results of the Al12Si alloy produced by low-pressure casting at different liquid metal velocities. The Weibull analysis of tensile strength and elongation at fracture clearly demonstrates that liquid metal velocity significantly influences both the mechanical performance and reliability of Al–Si alloy castings. At a liquid metal velocity of 0.25 m/s, the tensile strength distribution exhibits a very high Weibull modulus (m = 39.3), indicating extremely low

scatter and high reliability. This shows the importance of non-turbulent filling that eliminates bifilm entrainment, leading to high quality castings with lowest porosity. However, the relatively lower characteristic strength (β = 126.5 MPa) indicates that the load-bearing capacity remains limited under these conditions. This behaviour is attributed to the low liquid metal velocity (a near-stagnant liquid front), leading to slightly slower cooling in which the eutectic structure becomes relatively coarser (Fig. 3).

Table 5
Weibull analysis of tensile test results of Al12Si alloy produced by the low-pressure casting method at different liquid metal velocities.

Pressure (mbar)	Filling velocity (m/s)	Tensile strength		Elongation at fracture	
		Weibull modulus (m)	Weibull Characteristic (beta)	Weibull modulus (m)	Weibull Characteristic (beta)
80	0.25	39.3	126.5	10.6	4.5
125	0.5	11.5	150.1	16.8	4.6
200	1	10.7	131.8	6.4	3.9

Increasing the liquid metal velocity to 0.5 m/s results in a pronounced improvement in tensile performance, with the highest characteristic strength (β = 150.1 MPa) obtained. This enhancement is likely associated with improved feeding conditions and microstructural refinement due to increased cooling rates. Despite this improvement, the Weibull modulus decreases to m = 11.5, indicating a moderate increase in data scatter, likely due to the onset of flow instabilities during mould filling. The elongation results exhibit a similar trend. The specimens cast at 0.5 m/s show the highest Weibull modulus (m = 16.8) and characteristic elongation (β = 4.6%), indicating improved ductility and relatively consistent deformation behavior. In contrast, at 1 m/s, both the Weibull modulus (m = 6.4) and characteristic elongation (β = 3.9%) decrease significantly, reflecting increased variability and reduced ductility. It is important to note that 1 m/s filling rate has the lowest elongation at fracture between the studied velocities in this work. This is quite important because turbulent filling leads to oxide entrainment which radically deteriorates the toughness and soundness of the cast part. These defects act as critical stress concentrators and crack initiation sites, leading to premature failure and increased scatter in mechanical properties. Overall, the results indicate that while increasing filling velocity enhances the characteristic strength up to an optimal level, excessive velocity adversely affects both strength and ductility by reducing reliability. Therefore, a liquid metal velocity of 0.5 m/s provides the most favorable balance between mechanical performance and reliability for the casting conditions investigated. Figure 6 presents the survival probability distributions of the tensile strength (a) and elongation at fracture (b) of Al12Si alloy specimens produced by low-pressure die casting at different liquid-metal velocities. As shown in Fig. 6.a, the specimens produced at 0.5 m/s exhibited higher tensile strength. Similarly, the highest elongation at fracture was obtained at 0.5 m/s, as shown in Fig. 6. b. These results indicate that 0.5 m/s provides the most favorable mechanical properties.

Similar observations have been reported in the literature. Xiong et al. investigated the microstructural and mechanical properties of A357 alloy cast under vacuum-assisted counter-gravity conditions, analogous to low-pressure casting, at different temperatures (580–610°C). They found that the alloys cast at 590°C exhibited the highest density, along with the maximum yield and tensile strengths. They also observed a noticeable change in dendritic morphology and attributed this variation to differences between the liquidus and casting temperatures [23]. Fu et al. examined the effects of mould filling time, holding time under pressure, and casting temperature in determining the optimum processing conditions for AM50 magnesium alloy in a low-pressure casting system. Their results indicated that the best tensile properties were achieved with a filling time of 15–22 s, a pressure-holding time of 8–12 s, a casting temperature of 705–710°C, and a mould temperature of 390–410°C [24]. In another study, it was also reported that, for A356 alloys cast into both sand and metallic moulds using a low-pressure casting system, the highest tensile strength and ductility were achieved in the metallic mould [19]. Consistent with these findings, the density results from the present study showed that the highest density was achieved at a pressure of 0.125 bar, corresponding to a nozzle inlet velocity of 0.50 m/s.

Merlin et al. reported that casting defects become particularly critical when concentrated around the V-notch, as they reduce the effective load-bearing area of Charpy specimens. Therefore, the presence of such defects significantly influences impact properties and may overcome the effect of the microstructure [25]. Teng et al. reported that there was no direct correlation between pores and fractures [26], and Olofson explained why. Olofsson showed that bifilms are more important than pores as crack initiators [27]. Gyarmati et al. reported that computed tomography-aided porosity analysis of RPT samples can be used to quantify melt quality [28]. According to Nebreda, the effective bubble dispersion achieved by the high shear melt conditioning (HSMC) technology markedly reduces the presence of bifilms while promoting faster, more efficient degassing.

Furthermore, melt quality can be conveniently assessed using the reduced pressure test (RPT) [29]. Gürsoy et al., in the LPDC method, instead of pumping the liquid metal across the entire surface of the melting furnace, delivered it to the mould cavity using a pump. As a result, the melt quality of the A356 alloy deteriorated over time, resulting in increased porosity. This was attributed to the consumption of air between the folded oxides, increasing the oxide thickness of the bifilms layer. A relationship between the bifilm index and pore formation was found [30].

The macrohardness results of the Al12Si alloy produced by low-pressure casting at different liquid metal velocities are shown in Fig. 7. It was observed that macrohardness increased with increasing liquid metal velocity, with average values of 50 HB, 63 HB, and 66 HB for the alloys cast at 0.25, 0.50, and 1.00 m/s, respectively. This improvement is likely associated with variations in solidification conditions and the corresponding microstructural evolution. In support of this interpretation, Bedel et al. examined the influence of geometric changes in the transition region between the vertical runner and the mould cavity on liquid metal flow in low-pressure casting. They proposed several strategies to reduce bifilm formation through numerical and analytical analyses. Their results showed that, in the presence of cross-sectional

variation, increasing the height of the transition region reduced oscillation-induced surface turbulence of the liquid metal.

In contrast, the cross-sectional shape itself did not significantly affect the overall flow characteristics [31]. Han et al. reported that pressure holding time significantly affects the casting quality of wheel hubs. Cooling rate is important on SDAS and tensile [32].

4. Conclusion

In this study, the effects of different liquid metal velocities on the microstructural and mechanical properties of Al12Si alloy LPDC were evaluated, and the results are summarized below.

- OM and SEM analyses revealed that, due to the increasing liquid metal velocity, the Al dendrites morphologically transformed from linear-columnar dendrites to star-shaped dendrites, and the grain refinement effect thinned the Al-Si eutectic. Furthermore, there was a significant decrease in porosity.
- According to the tensile test results, the highest average tensile strength was obtained in the Al12Si alloy cast at a liquid metal velocity at the gate of 0.50 m/s, and the lowest average tensile strength was obtained in the Al12Si alloy cast at a a liquid metal velocity at the gate of 0.25 m/s.
- According to the macrohardness results, macrohardness increases approximately 32% with increasing liquid metal velocity. This behavior is attributed to the more rapid filling of the mould cavity and the higher cooling rates associated with the increased liquid metal velocity.
- The Weibull analysis demonstrated that a low filling velocity (0.25 m/s) results in a significantly higher Weibull modulus, indicating superior reliability due to reduced turbulence and minimized defect formation; however, due to slow solidification and a coarse microstructure, it also reveals the lowest mechanical properties.
- The critical filling velocity (0.5 m/s) provides the highest characteristic strength and elongation; on the other hand, an excessive filling velocity (1 m/s) leads to a marked decrease in both the Weibull modulus and mechanical performance, owing to turbulence-induced defects such as bifilms and porosity.

Declarations

Declaration of ethical standards

The author(s) of this article declare that the materials and methods used in their study did not require ethical committee approval and/or any legal or special permission.

Conflict of interest

There is no conflict of interest in this study.

Author Contribution

T.T. conceived and supervised the study and contributed to the experimental design and interpretation of the results. A.C. performed the casting experiments, sample preparation, and mechanical and microstructural characterisation and prepared the figures and tables. D.D. contributed to the casting methodology, melt-quality assessment, Weibull analysis, and interpretation of casting defects. T.T. and A.C. wrote the initial draft of the manuscript. All authors reviewed and approved the final manuscript.

Acknowledgements

The authors would like to thank the Scientific Research Projects Coordination Unit of Karabük University for supporting this research under Project No. KBÜBAP-22-YL-154.

Data Availability

The datasets generated and/or analysed during the current study are available from the corresponding author upon reasonable request.

References

1. Campbell J (2011) Complete Casting Metal Casting Processes, Metallurgy, Techniques and Design, First edit. Butterworth-Heinemann, Oxford
2. Jarfors AEW, Seifeddine S, Metal casting (2015) https://doi.org/10.1007/978-1-4471-4670-4_81
3. Campbell J (2003) Casting
4. Bonollo F, Urban J, Bonatto B, Botter M (2005) Gravity and Low pressure die casting of aluminium alloys: A technical and economical benchmark. Metall Ital 97:23–32
5. Campbell J (2006) Entrainment defects. Mater Sci Technol 22:127–145. https://doi.org/10.1179/174328406X74248
6. Zhang B, Cockcroft SL, Maijer DM, Zhu JD, Phillion AB (2005) Casting defects in low-pressure die-cast aluminum alloy wheels. Jom 57:36–43. https://doi.org/10.1007/s11837-005-0025-1
7. Du D, An J, Dong A, Sun B (2025) A review of the progress and challenges of counter-gravity casting. J Mater Sci Technol 216:1–26. https://doi.org/10.1016/j.jmst.2024.07.037
8. Kheirabi A, Baghani A, Bahmani A, Tamizifar M, Davami P, Ostad Shabani M, Mazahery A (2018) Understanding the occurrence of the surface turbulence in a nonpressurized bottom gating system: Numerical simulation of the melt flow pattern, Proc. Inst. Mech. Eng. Part L J. Mater. Des. Appl. 232 230–241. https://doi.org/10.1177/1464420715621930
9. Dai X, Jolly M, Yang X, Campbell J (2012) Modelling of liquid metal flow and oxide film defects in filling of aluminium alloy castings, IOP Conf. Ser Mater Sci Eng 33. https://doi.org/10.1088/1757-

899X/33/1/012073

10. Qiu Z, Zhang C, Zhang L, Cao F, Shen H, Jin Z, Cao G, Zhao X, Song H, Sun J (2024) Revealing the Relationship between Critical Inlet Velocity and a Double-Layer Oxide Film Combined with Low-Pressure Casting Technology. J Manuf Mater Process 8. https://doi.org/10.3390/jmmp8040168
11. Song H, Zhang L, Cao F, Gu X, Sun J (2021) Oxide bifilm defects in aluminum alloy castings. Mater Lett 285. https://doi.org/10.1016/j.matlet.2020.129089
12. Sun J, Le Q, Fu L, Bai J, Tretter J, Herbold K, Huo H (2019) Gas entrainment behavior of aluminum alloy engine crankcases during the low-pressure-die-casting process. J Mater Process Technol 266:274–282. https://doi.org/10.1016/j.jmatprotec.2018.11.016
13. Yang X, Huang X, Dai X, Campbell J, Tatler J (2004) Numerical modelling of entrainment of oxide film defects in filling of aluminium alloy castings. Int J Cast Met Res 17:321–331. https://doi.org/10.1179/136404604225022748
14. Ou J, Wei C, Cockcroft S, Maijer D, Zhu L, Lateng A, Li C, Zhu Z (2020) Advanced process simulation of low pressure die cast a356 aluminum automotive wheels— part i, process characterization. Met (Basel) 10. https://doi.org/10.3390/met10050563
15. Ou J, Wei C, Cockcroft S, Maijer D, Zhu L, Lateng A, Li C, Zhu Z (2020) Advanced process simulation of low pressure die cast a356 aluminum automotive wheels—part ii modeling methodology and validation. Met (Basel) 10:1–24. https://doi.org/10.3390/met10111418
16. Li S, Han J, Wang J, Liu D, Guo S, Bi J, Dong G (2025) Defects and fatigue properties of LPDC-fabricated aluminum alloy wheel: Experimental and numerical simulation methods. Eng Fail Anal 182:110074. https://doi.org/10.1016/j.engfailanal.2025.110074
17. Puga H, Barbosa J, Azevedo T, Ribeiro S, Alves JL (2016) Low pressure sand casting of ultrasonically degassed AlSi7Mg0. 3 alloy : Modelling and experimental validation of mould fi lling. JMADE 94:384–391. https://doi.org/10.1016/j.matdes.2016.01.059
18. Timelli G, Caliari D, Rakhmonov J (2016) Influence of Process Parameters and Sr Addition on the Microstructure and Casting Defects of LPDC A356 Alloy for Engine Blocks. J Mater Sci Technol 32:515–523. https://doi.org/10.1016/j.jmst.2016.03.010
19. Chiesa F, Duchesne B, Marin G (2020) Low-Pressure Casting of Aluminium AlSi7Mg03 (A356) in Sand and Permanent Molds. MATEC Web Conf 326:06001. https://doi.org/10.1051/matecconf/202032606001
20. Papanikolaou M, Saxena P, Pagone E, Salonitis K, Jolly M (2020) Optimisation of the filling process in counter-gravity casting, IOP Conf. Ser Mater Sci Eng 861. https://doi.org/10.1088/1757-899X/861/1/012031
21. Papanikolaou M, Pagone E, Georgarakis K, Rogers K, Jolly M, Salonitis K (2018) Design optimisation of the feeding system of a novel counter-gravity casting process. Met (Basel) 8:1–12. https://doi.org/10.3390/met8100817
22. Yousefian P, Tiryakioğlu M (2018) Pore Formation During Solidification of Aluminum: Reconciliation of Experimental Observations, Modeling Assumptions, and Classical Nucleation Theory. Metall

Mater Trans A 49:563–575. https://doi.org/10.1007/s11661-017-4438-6

23. Xiong B, Lin X, Wang Z, Yan Q, Yu H (2014) Microstructures and mechanical properties of vacuum counter-pressure casting A357 alloys solidified under grade-pressurising: Effects of melt temperature. Mater Sci Eng A 611:9–14. https://doi.org/10.1016/j.msea.2014.05.035
24. Fu P, Luo AA, Jiang H, Peng L, Yu Y, Zhai C, Sachdev AK (2008) Low-pressure die casting of magnesium alloy AM50: Response to process parameters. J Mater Process Technol 205:224–234. https://doi.org/10.1016/j.jmatprotec.2007.11.111
25. Merlin M, Timelli G, Bonollo F, Garagnani GL (2009) Impact behaviour of A356 alloy for low-pressure die casting automotive wheels. J Mater Process Technol 209:1060–1073. https://doi.org/10.1016/j.jmatprotec.2008.03.027
26. Teng X, Mae H, Bai Y, Wierzbicki T (2009) Pore size and fracture ductility of aluminum low pressure die casting. Eng Fract Mech 76:983–996. https://doi.org/10.1016/j.engfracmech.2009.01.001
27. Olofsson J, Bogdanoff T, Tiryakioğlu M (2024) On the Competition between Pores and Hidden Entrainment Damage during In Situ Tensile Testing of Cast Aluminum Alloy Components, Metals (Basel). 14 https://doi.org/10.3390/met14101175
28. Gyarmati G, Fegyverneki G, Mende T, Tokár M (2019) Characterization of the double oxide film content of liquid aluminum alloys by computed tomography. Mater Charact 157:109925. https://doi.org/10.1016/j.matchar.2019.109925
29. Lazaro-Nebreda J, Patel JB, Fan Z (2021) Improved degassing efficiency and mechanical properties of A356 aluminium alloy castings by high shear melt conditioning (HSMC) technology. J Mater Process Technol 294:117146. https://doi.org/10.1016/j.jmatprotec.2021.117146
30. Gursoy O, Nordmak A, Syvertsen F, Colak M, Tur K, Dispinar D (2021) Role of metal quality and porosity formation in low pressure die casting of A356: Experimental observations. Arch Foundry Eng 21:5–10. https://doi.org/10.24425/afe.2021.136071
31. Bedel M, Sanitas A, Mansori ME (2019) Geometrical effects on filling dynamics in low pressure casting of light alloys. J Manuf Process 45:194–207. https://doi.org/10.1016/j.jmapro.2019.06.006
32. Han J, Dong G, Li S, Zheng J, Wang J, Li H, Starostenkov MD, Bi J (2024) Uneven distribution of cooling rate, microstructure and mechanical properties for A356-T6 wheels fabricated by low pressure die casting. J Manuf Process 127:196–210. https://doi.org/10.1016/j.jmapro.2024.08.001

Figures



Fig. 1 Photographic view of the low-pressure casting machine

Figure 1

See image above for figure legend

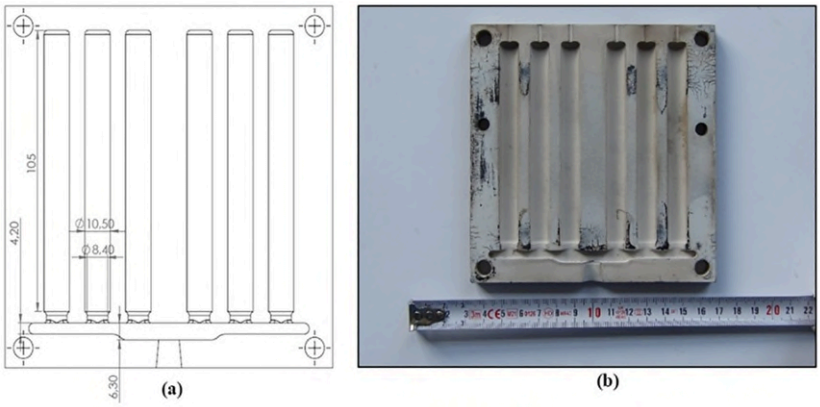


Fig. 2 Metal mould dimensions (a) and metal mould photograph (b).

Figure 2

See image above for figure legend

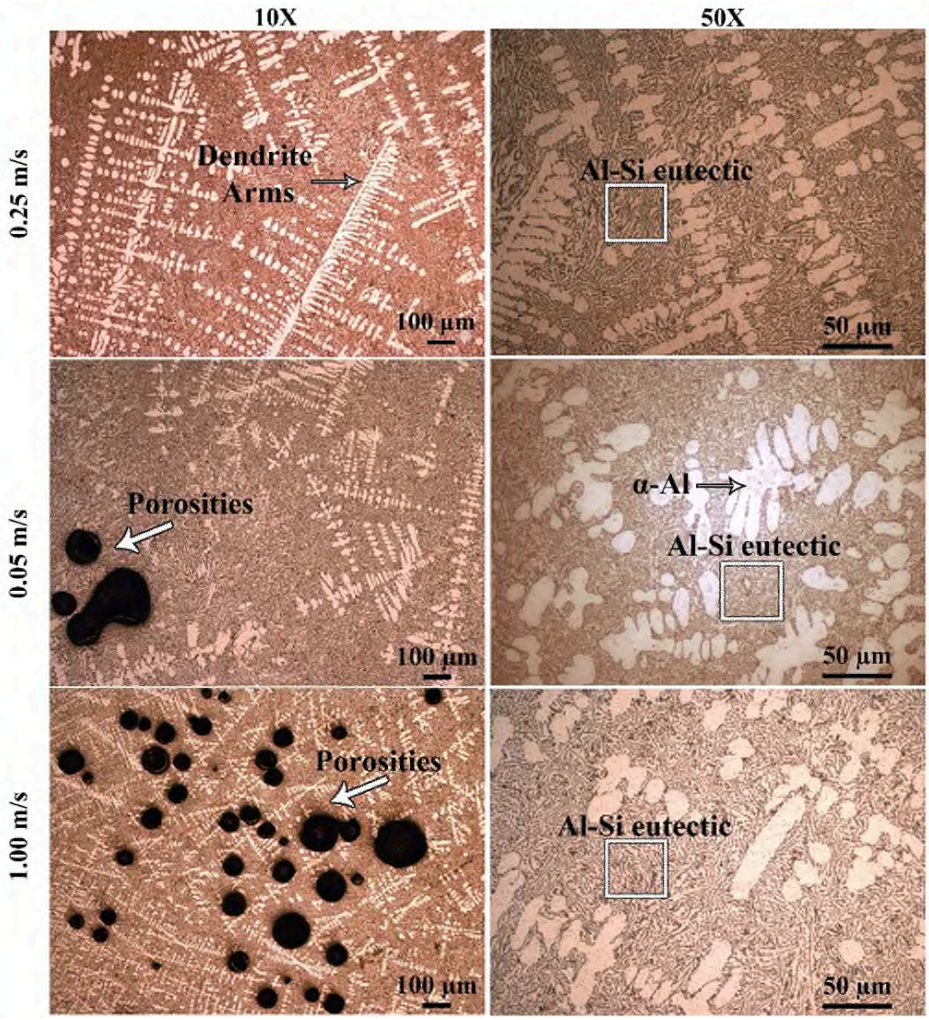


Fig. 3 OM images of Al12Si alloy produced by the low-pressure casting method at different liquid metal velocities.

Figure 3

See image above for figure legend

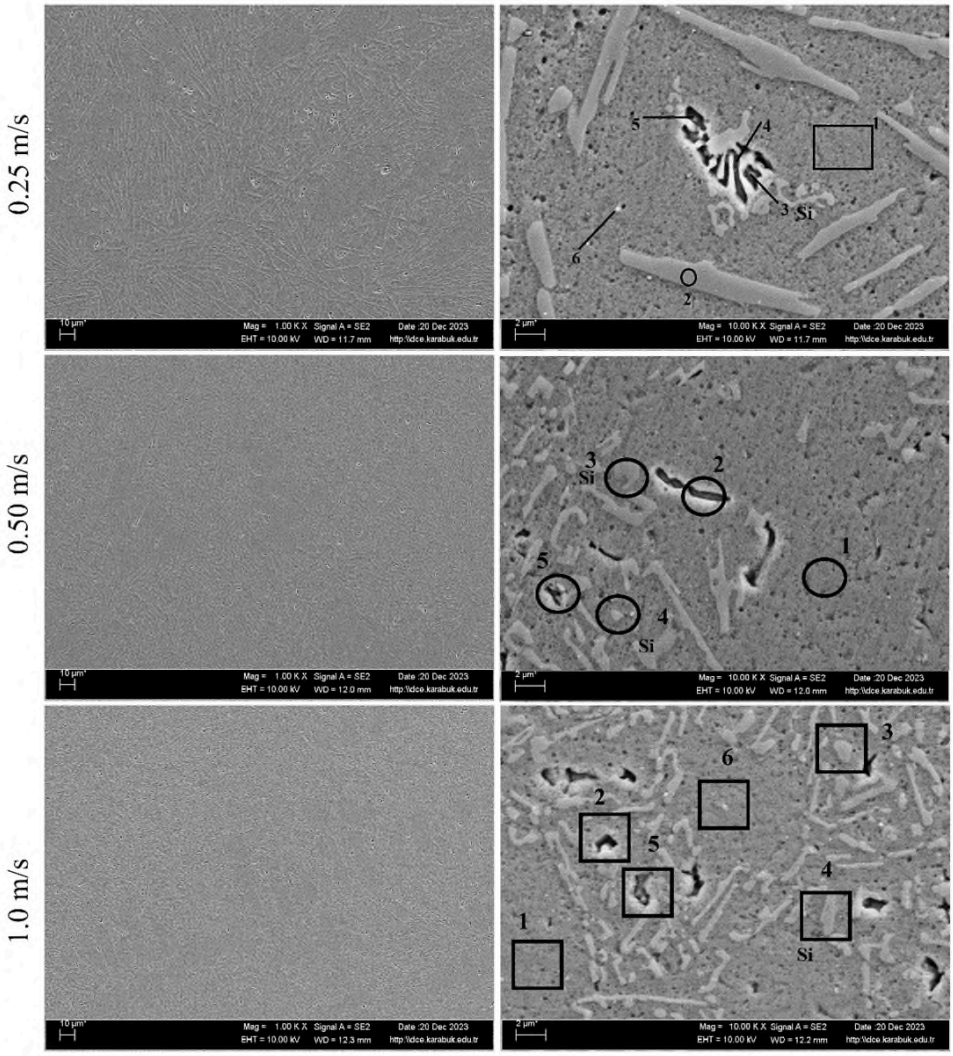


Fig. 4 SEM images of Al12Si alloy produced by the low-pressure casting method at different liquid metal velocities.

Figure 4

See image above for figure legend

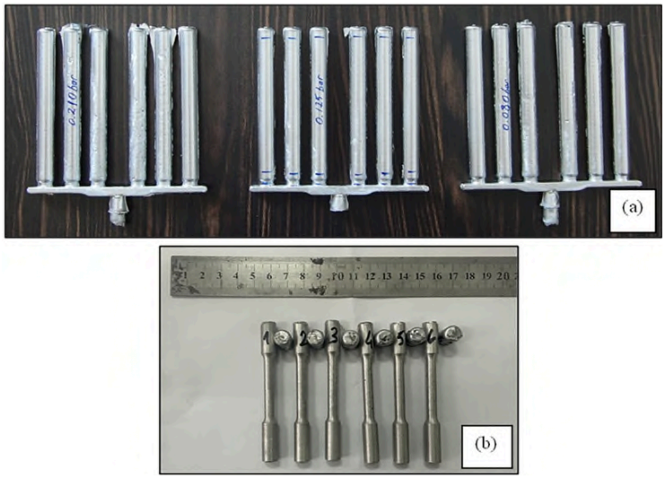


Fig. 5 Al12Si alloy specimens produced by the low-pressure casting method at different liquid metal velocities (a) and tensile test specimens (b).

Figure 5

See image above for figure legend

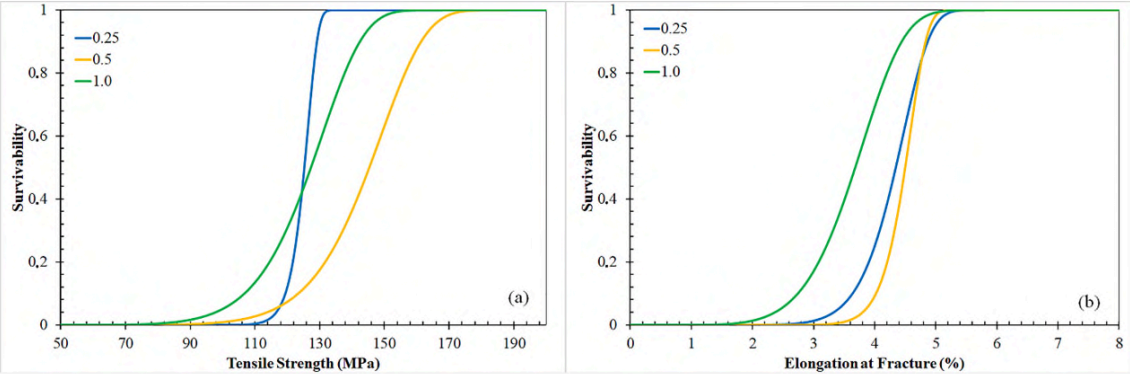


Fig. 6 Al12Si alloy specimens produced by the low-pressure casting method at different liquid metal velocities, survivability of tensile strength (a), and survivability of elongation at fracture (b).

Figure 6

See image above for figure legend

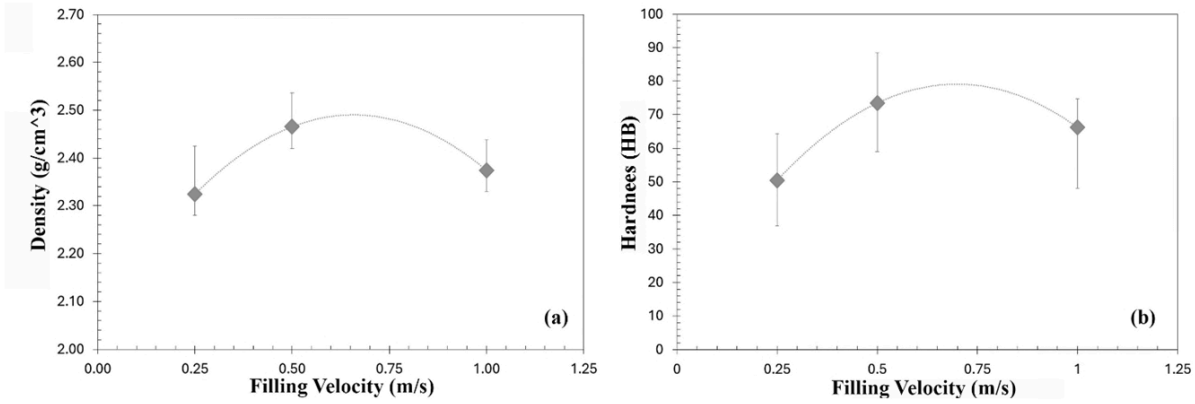


Fig. 7 Macro hardness results (a) and distributions (b) of Al12Si alloy produced by LPDC at low pressures at different liquid metal velocities.

Figure 7

See image above for figure legend

Supplementary Files

This is a list of supplementary files associated with this preprint. Click to download.

- SHighlights.docx